Research
Intelligent Manufacturing—Article

# Human–Robot Collaboration Framework Based on Impedance Control in Robotic Assembly

Xingwei Zhao, Yiming Chen, Lu Qian, Bo Tao *, Han Ding

*State Key Laboratory of Digital Manufacturing Equipment and Technology, School of Mechanical Science and Engineering, Huazhong University of Science and Technology, Wuhan 430074, China*

A B S T R A C T

Human–robot (HR) collaboration (HRC) is an emerging research field because of the complementary advantages of humans and robots. An HRC framework for robotic assembly based on impedance control is proposed in this paper. In the HRC framework, the human is the decision maker, the robot acts as the executor, while the assembly environment provides constraints. The robot is the main executor to perform the assembly action, which has the position control, drag and drop, positive impedance control, and negative impedance control modes. To reveal the characteristics of the HRC framework, the switch condition map of different control modes and the stability analysis of the HR coupled system are discussed. In the end, HRC assembly experiments are conducted, where the HRC assembly task can be accomplished when the assembling tolerance is 0.08 mm or with the interference fit. Experiments show that the HRC assembly has the complementary advantages of humans and robots and is efficient in finishing complex assembly tasks.

## 1. Introduction

Human–robot (HR) collaboration (HRC) is an emerging research field because of the complementary advantages of humans and robots [1]. Humans are good with self-adaption with the instructed environment, whereas robots are good in execution with an accuracy performance [2–4]. Compared with a human or robot working alone, an HR team is more efficient and flexible [5,6].

Robot assembling processes face flexibility and adaptability assembly tasks because of customized products. Robot along is hard to accomplish customized products assembling. In contrast, a human-guided assembly with the robot assistance has advantages compared with a full automation assembly [7]. Different HRC modes have been studied in the HR assembling line. HRC can improve the intelligence of complex assembly processes [5]. Ding et al. [6] studied the work mode of the hybrid HR cell, which could improve the efficiency of the assembling line. Bonilla and Asada [8] developed wearable robotic limbs to assist manufacturing. In the Bavarian Motor Works (BMW)'s factory, the robot cooperates with a human worker to insulate vehicle doors [9]. To

mount a gear into a square-section shaft, Roveda et al. [10] proposed a sensorless impedance control to enhance the uncertainty adaptation of the robot. Jiang et al. [11] reviewed the robot control for high-tolerance peg-in-hole assembly task, where impedance control and hybrid force/position control were mainly used in the assembly. Realyvásquez-Vargas et al. [12] stated that the implementation of collaborative robots in assembly station could reduce the employees' incidence of occupational risks.

In general, the HRC mode includes human tutor mode or leader–follower mode, where the human is in a primary role. The human tutor mode aims to transfer human skills to a robot according to the demonstration [13,14]. Aside from motion, human impedance can be also transferred to robots [15]. Yang et al. [16] developed a control strategy that a robot can learn the movement and stiffness features from the human tutor. Robot assistance mode aims to help humans toward smooth and intuitive reactive behavior [17], such as gravity compensation of heavy load [18] or impedance compensation [19]. With the improvement of the control technique, robots can also play an adaptive and primary role in leading a task [20]. Musić and Hirche [21] studied control sharing in HR team interaction, which focused on the questions of HRC decision-making to improve the task execution capabilities. Khoramshahi and Billard [22] proposed a task-adaptation approach

---

* Corresponding author.
  *E-mail address:* taobo@mail.hust.edu.cn (B. Tao).

in physical HR interaction (HRI), where robots could intelligently adapt the motions following the human intention in a multi-task setting. To optimize the task sequence allocation scheme in the assembly processes, Zhang et al. [23] studied a collaborative reinforcement learning algorithm, where the assembly task could be assigned to robots or humans based on the task complexity.

With respect to the control method, the impedance control is widely used in HRC, which can provide stable tracking by regulating the impedance response of a robot when the robot contacts the external environment [24–26]. Burdet et al. [27] stated that the human central nervous system acts similar to an impedance controller, which can ensure the stability and reject disturbances by increasing the impedance. Motivated by this, Li et al. [28] designed an adaptive impedance controller for robots that could adapt feedforward force, impedance, and reference trajectory. Chen et al. [29] proposed HR impedance mapping to realize an effective execution of HRC, where the impedance of the robot arm was compliant to the human arm impedance. Roveda et al. [30] proposed a model-based reinforcement learning strategy for the impedance control in HRC tasks. Later, Zhao et al. [31] proposed model-based actor–critic learning algorithm to find the optimal impedance control during HRI, where a safety-learning strategy was designed to train the robot in safety environment.

A general framework for HRI/HRC, which combines different control technique into a framework solution, is also an appealing topic. To build an HRI framework, differential game theory has been used to describe various HRI [32]. Later, Li et al. [33] designed the HRI control strategy model based on the cost functions in game theory framework. By varying the cost function, the HRI relationship can be classified into cooperation, collaboration, and competition [33]. HRC is a sub-field of the HRI, in which robots are designed to share space and tasks with human [34]. Mukherjee et al. [35] reviewed the robot learning strategies for HRC, where a taxonomy of the levels of HRI has been presented. In this taxonomy, the HRC is in the level 4 which is the key step to the final level (i.e. the fully autonomous level) [35]. Xing et al. [36] presented a learning from demonstration strategy for HRC, where the robot follows the user's intention by imitating the movement of humans. Kim et al. [37] presented an HRC framework that considered the ergonomic aspects of the human co-worker. Peternel et al. [38] proposed an HRC framework, where the robot behavior was adapted to the human motor fatigue. Gopinath et al. [39] studied the safety criterion for HRC assembling. An extensive literature review of HRC has been published. Villani et al. [40] reviewed the HRC framework with specific focus on physical and cognitive HRIs. Ajoudani et al. [41] reviewed the intermediate HR interfaces for HRC, including the HRI modalities, the control performances, and the HRI benchmarking. A general framework to evaluate HRC with human-social factors is reviewed by Gervasi et al. [34]. Matheson et al. [42] reviewed the HRC in manufacturing applications, and presented the related standards and modes of the HRC. Liu and Wang [43] reviewed the gesture recognition for HRC, in which the gesture recognition was considered the strong interface between humans and robots.

Given that the HRC framework is widely studied, a general HRC framework based on impedance control for the robotic assembly is missing. As the force interaction is the key point in the assembly scenario, a framework for HRC that derives from impedance control in robotic assembly is studied in this paper. As a characteristic of the impedance control, adjusting the state feedback and force feedback gains to achieve different impedance properties is possible. By doing this, four different control modes can be obtained, in terms of robot position control, robot drag and drop, positive impedance mode, and negative impedance mode. Then, the HRC framework is built up based on the four control modes. Even though such control modes may be studied separately in different HRC scenar-

ios, our contribution is to design the negative impedance control mode and complete the HRC framework in robot assembling. As deriving from impedance control, our HRC framework is easy to execute in the robot system. Experiments show the implementation of the HRC framework into a robot system, and the HRC assembly task can be accomplished when the assembling tolerance is 0.08 mm or with the interference fit.

The remainder of the paper is organized as follows. Section 2 presents the HRC framework. Section 3 studies the switch condition map during HRC and the stability analysis of the HR coupled system. Section 4 provides simulation to show the robot response under the different control modes. Section 5 presents the experimental investigation. Finally, Section 6 presents the concluding remarks.

## 2. The framework for HRC in robotic assembly

In HRC, human provides sensory-motor capabilities and problem-solving skills; robots show high repeatability, speed, and load ability; and the HRC team could potentially increase productivity [44]. As the interaction force plays important role during assembly task, there are some assumptions to the HRC for robotic assembly:

(1) For the human, we assume that the human worker is intelligent and well trained. The human worker should know the assembling process, assembling constraint, and other assembling knowledge.

(2) For the robot, the robot action should be deterministic and predictable. The input–output relation of the robot should be as simple as possible and must be known by the human worker.

(3) For HRC, the complex programming during assembling should be avoided. The human intention should be transmitted to the robots by the interaction force or simple command.

Based on the assumptions, our HRC framework is defined as follows. In the HRC, the human is the decision maker, the robot acts as the executor, whereas the assembly environment provides constraints. The robot is the main executor to perform the assembly action, which has the position control, drag and drop, positive impedance control, and negative impedance control modes. The four modes indicate the different behaviors of the robot with respect to the interaction force. For a specific assembling task, the human can treat the robot as a reliable companion. The human collaborates with the robot by selecting suitable control modes and leads the robot to comply or confront the environment. The assembly tasks are finally accomplished by the HR team. During HRC assembly, interaction force connects the human, the robot, and the environment. On the one hand, the human intention transmits to the robot by the interaction force. On the other hand, the interaction force between the robot and workpiece indicates the assembly constraint. The framework for HRC based on impedance control is given in Fig. 1.

Under the HRC framework, the different control modes are presented, in terms of the position control, drag and drop, positive impedance control, and negative impedance control modes.

The original dynamic model of robots in the Cartesian space [45] can be written as

$$M_R(\boldsymbol{x}_R)\ddot{\boldsymbol{x}}_R + C_R(\boldsymbol{x}_R, \dot{\boldsymbol{x}}_R)\dot{\boldsymbol{x}}_R + G_R(\boldsymbol{x}_R) = \boldsymbol{J}^{-T}\boldsymbol{\tau}_R + \boldsymbol{F}$$
$$\boldsymbol{x}_R = [x \quad y \quad z \quad \alpha \quad \beta \quad \gamma]^T \tag{1}$$

where $\boldsymbol{x}_R$, $\dot{\boldsymbol{x}}_R$, and $\ddot{\boldsymbol{x}}_R$ is the position, speed, and acceleration of the robot in Cartesian space, respectively; $M_R(\boldsymbol{x}_R)$ is the mass matrix; $C_R(\boldsymbol{x}_R, \dot{\boldsymbol{x}}_R)$ is the damping matrix; $G_R(\boldsymbol{x}_R)$ is the gravity force; $\boldsymbol{\tau}_R$ is the input torque; $\boldsymbol{F}$ is external force; $\boldsymbol{J}$ represents the Jacobian matrix; $x$, $y$, and $z$ are the translational positions of the robot; and $\alpha$, $\beta$, and $\gamma$ are the rotational positions of the robot.

**Fig. 1.** HRC framework based on impedance control, where the human is the decision maker, the robot acts as the executor, and the assembly environment provides constraints.

By compensating the nonlinear terms, the acceleration control of the robot $\ddot{\boldsymbol{x}}_R$ in Cartesian space is

$$\ddot{\boldsymbol{x}}_R = -\boldsymbol{K}_{R,p}(\boldsymbol{x}_R - \boldsymbol{x}_{R,r}) - \boldsymbol{K}_{R,d}\dot{\boldsymbol{x}}_R + \boldsymbol{K}_{R,f}\boldsymbol{F} \tag{2}$$

where $\boldsymbol{x}_{R,r}$ is the desired trajectory; $\boldsymbol{K}_{R,p}$, $\boldsymbol{K}_{R,d}$, and $\boldsymbol{K}_{R,f}$ are the position, speed, and force feedback of the robot, respectively. The way to obtain Eq. (2) from Eq. (1) is shown in Appendix A.

The dynamic model of the human arm is similar to the robot arm, and the acceleration of the human arm $\ddot{\boldsymbol{x}}_H$ is

$$\ddot{\boldsymbol{x}}_H = -\boldsymbol{K}_{H,p}(\boldsymbol{x}_H - \boldsymbol{x}_{H,r}) - \boldsymbol{K}_{H,d}\dot{\boldsymbol{x}}_H + \boldsymbol{K}_{H,f}\boldsymbol{F} \tag{3}$$

where $\boldsymbol{x}_H$ and $\dot{\boldsymbol{x}}_H$ are the joint position and speed of the human arm, respectively; $\boldsymbol{x}_{H,r}$ is the desired position of the human arm; $\boldsymbol{K}_{H,p}$, $\boldsymbol{K}_{H,d}$, and $\boldsymbol{K}_{H,f}$ are the position, speed, and force feedback of the human arm, respectively.

The force is generated by the interaction behavior within the human arm and the robot arm, where the interactive stiffness mainly influences the interaction force

$$\boldsymbol{F} = \boldsymbol{K}_{HR}(\boldsymbol{x}_R + \boldsymbol{x}_H) \tag{4}$$

where $\boldsymbol{K}_{HR}$ is the stiffness and damping of HRI.

Substituting Eq. (4) into Eq. (2), the interaction force of the robot in the equilibrium position is written as

$$\boldsymbol{F} = \boldsymbol{K}_{R,f}^{-1}\boldsymbol{K}_{R,p}(\boldsymbol{x}_{R,eq} - \boldsymbol{x}_{R,r}) \tag{5}$$

where $\boldsymbol{K}_{R,f}^{-1}\boldsymbol{K}_{R,p}$ indicates the equivalent stiffness of the robot under impedance control; $\boldsymbol{x}_{R,eq}$ is the equilibrium position of the robot in Cartesian space. By changing $\boldsymbol{K}_{R,f}$ and $\boldsymbol{K}_{R,p}$, four control modes can be obtained.

**Mode I: position control.** Robot position control mode is widely used in the robot control mode. In this case,

$$\boldsymbol{K}_{R,p} > 0, \boldsymbol{K}_{R,f} \approx 0 \tag{6}$$

then

$$\begin{aligned} \boldsymbol{F} &= \boldsymbol{K}_{R,f}^{-1}\boldsymbol{K}_{R,p}(\boldsymbol{x}_{R,eq} - \boldsymbol{x}_{R,r}) \\ \boldsymbol{K}_{R,f}^{-1} &\to \infty \\ \boldsymbol{x}_{R,eq} &\approx \boldsymbol{x}_{R,r} \end{aligned} \tag{7}$$

Given that $\boldsymbol{K}_{R,f}$ approaches zero and $\boldsymbol{K}_{R,p}$ has large value, the robot system has large stiffness, and $\boldsymbol{x}_{R,eq}$ is almost equal to $\boldsymbol{x}_{R,r}$.

**Mode II: drag and drop.** Drag and drop mode is widely used in HRC, where the human can import the trajectory to the robot by demonstration. In this case,

$$\boldsymbol{K}_{R,p} = 0, \ \boldsymbol{K}_{R,f} > 0 \tag{8}$$

Given that $\boldsymbol{K}_{R,p} = 0$, we have $\boldsymbol{F} = 0$.

In this case, the robot moves in the direction of the interaction force and stops when the interaction force equals zero.

**Mode III: positive impedance control.** In positive impedance control mode, the robot acts as a spring, and regulates the impedance response when the robot contacts the external obstacle,

$$\boldsymbol{K}_{R,p} > 0, \ \boldsymbol{K}_{R,f} > 0 \tag{9}$$

then

$$\boldsymbol{F} = \boldsymbol{K}_{R,f}^{-1}\boldsymbol{K}_{R,p}(\boldsymbol{x}_{R,eq} - \boldsymbol{x}_{R,r}) \tag{10}$$

In this case, the external force results in a deviation of the robot from its desired position.

**Mode IV: negative impedance control.** In negative impedance control mode, the force feedback has opposite sign to the positive impedance control.

$$\boldsymbol{K}_{R,p} > 0, \ \boldsymbol{K}_{R,f} < 0, \ \boldsymbol{x}_{R,r} = 0 \tag{11}$$

and

$$\boldsymbol{F} = \boldsymbol{K}_{R,f}^{-1}\boldsymbol{K}_{R,p}\boldsymbol{x}_{R,eq} \tag{12}$$

Noticeable, in Mode IV, the interaction system may be unstable, and $\boldsymbol{x}_{R,eq}$ may not exist. In this way, the robot moves in the opposite direction of the interaction force.

Modes I–IV are four basic robot control modes. Modes I and II are basic functions of collaborative robots. Mode III is the impedance control, which is widely studied in literature, where the control gain could be a constant, nonlinear [25], or adaptive function [15]. Mode IV is rarely used in robot control because it may result in instability. However, in this paper, this mode is used to generate a large impulse force, which is meaningful in some assembling situations. Fig. 2 shows the classification of different control modes, where the x-axis is the force feedback, and the y-axis is the state feedback. By varying the force feedback, the control mode is varied within I to IV.

A switch parameter $\theta_{mod}$ is used to define the control modes. The control can be written as

$$\begin{aligned} \boldsymbol{K}_{R,p} &= \boldsymbol{K}_{nor}\sin\theta_{mod} \\ \boldsymbol{K}_{R,f} &= \boldsymbol{K}_{nor}\cos\theta_{mod} \\ \boldsymbol{K}_{nor} &= \textbf{diag}[K_{nor,1}, ..., K_{nor,i}, ..., K_{nor,6}] \\ \sin\theta_{mod} &= \textbf{diag}[\sin\theta_{mod,1}, ..., \sin\theta_{mod,i}, ..., \sin\theta_{mod,6}] \\ \cos\theta_{mod} &= \textbf{diag}[\cos\theta_{mod,1}, ..., \cos\theta_{mod,i}, ..., \cos\theta_{mod,6}] \end{aligned} \tag{13}$$

where $\boldsymbol{K}_{nor}$ is the matrix of the amplitude of the feedback gain; $K_{nor,i}$ is the amplitude of the feedback gain in $i$th directions; while $\theta_{mod,i}$ is the control mode in $i$th direction; **diag** indicates the diagonal matrix. The control mode is defined by the switch parameter as

$$\begin{cases} \text{Mode I}: \theta_{mod,i} \in [\pi/2 - \varepsilon, \pi/2) \\ \text{Mode II}: \theta_{mod,i} \in [0, \varepsilon) \\ \text{Mode III}: \theta_{mod,i} \in [\varepsilon, \pi/2 - \varepsilon) \\ \text{Mode IV}: \theta_{mod,i} \in [\pi/2, \pi) \end{cases} \tag{14}$$

where $\varepsilon$ is a small value. Then, the adjusting control mode is equivalent to adjusting the switch parameter $\theta_{mod,i}$.

The control mode for HRI can be further transformed into robot–environment interaction. The difference between humans
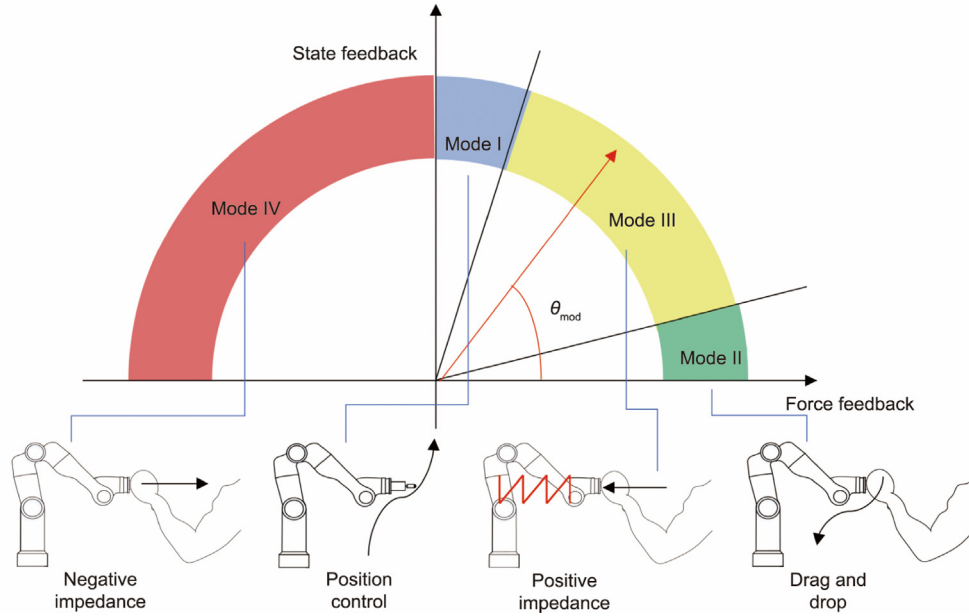
**Fig. 2.** Classification of different control modes.

and environment is that the desired position of the latter is the constraint position. Thus, the dynamics of the environment $\ddot{\boldsymbol{x}}_E$ is

$$\ddot{\boldsymbol{x}}_E = -\boldsymbol{K}_{E,p}(\boldsymbol{x}_E - \boldsymbol{x}_{E,r}) - \boldsymbol{K}_{E,d}\dot{\boldsymbol{x}}_E + \boldsymbol{K}_{E,f}\boldsymbol{F} \tag{15}$$

where $\boldsymbol{x}_{E,r}$ is the constraint position; $\boldsymbol{x}_E$ and $\dot{\boldsymbol{x}}_E$ are the joint position and speed of the environment, respectively; $\boldsymbol{K}_{E,p}$, $\boldsymbol{K}_{E,d}$, and $\boldsymbol{K}_{E,f}$ are the position, speed, and force feedback of the environment, respectively. The interaction force

$$\boldsymbol{F} = \boldsymbol{K}_{RE}(\boldsymbol{x}_R + \boldsymbol{x}_E) \tag{16}$$

where $\boldsymbol{K}_{RE}$ is the stiffness of the environment. Table 1 shows the classification of control mode during HRC or robot–environment interaction.

## 3. Switch condition and stability analysis of HRC

In this part, the switch conditions of different control modes during HRC are studied. When the robot interacts with the human arm, the stability of the coupled system is analyzed.

**Switch condition map.** Following the proposed HRC framework, the human can select various control modes under different interactive situations. A switch condition map is therefore proposed to assist human during HRC, as shown in Fig. 3. The switch mode can be concluded as trajectory learning, workspace limitation, safety principle, force requirement, task requirement, and so on.

- Trajectory learning. Modes I and II are generally used together. As a characteristic of collaborative robots, the human can import the trajectory with drag and drop in Mode II, and the robot repeats the demonstrated trajectory.
- Workspace limitation. If the workspace of the robot is bounded, the drag and drop modes should be limited when the boundary is reached. Thus, near the boundary of the work-

space, the control mode is changed from Mode IV to III. When the robot reaches the boundary, the control mode can be further switched to Mode IV or I. In Mode I, the robot will stay on the boundary. In Mode IV, the interaction force pushes the human arm from the boundary.
- Safety principle. the safety principle is to limit the interaction force. The mode switch chain is I → III → II, IV → III → II, or IV → II. When the external force is larger than a critical value, the robot should reduce its stiffness. Thus, the robot is from negative stiffness to positive stiffness and finally to zero stiffness.
- Force requirement. When high impulse interaction force is required, the robot can be controlled by Mode IV. Once the required force is reached, the robot should switch to Mode II or I rapidly. In this way, the impulse interaction force can be generated.
- Task requirement. Considering that the four control modes are the basic elements of HRC, the user can switch them arbitrarily with the task requirement.

To avoid the impact force during mode switch, a fuzzy switch law can be defined as

$$\ddot{\boldsymbol{x}}_R = \boldsymbol{K}_{nor}[-\sin\theta_{mod}\ (\boldsymbol{x}_R - \boldsymbol{x}_{R,r}) + \cos\theta_{mod}\ \boldsymbol{F}] - \boldsymbol{K}_{R,d}\dot{\boldsymbol{x}}_R \tag{17}$$

If the system is from the current mode $\theta_{mod,old}$ to the new mode $\theta_{mod,new}$, then the switch parameter $\theta_{mod}$ is

$$\theta_{mod}(t) = \theta_{mod,old} + \mu(t)\left(\theta_{mod,new} - \theta_{mod,old}\right), \mu(t) = \frac{t}{T} \tag{18}$$

where $\mu(t)$ is the fuzzy parameter $\mu$ at time $t$ and $\mu \in [0, 1]$; $T$ is the switch time duration.

**System stability analysis.** When robots interact with humans, the stability of the HR system depends on the coupled dynamics [46]. The robot and human arm dynamics can be written together as

$$\dot{\boldsymbol{X}}_i = \boldsymbol{A}_i\boldsymbol{X}_i + \boldsymbol{E}_i\boldsymbol{X}_{r,i}$$

$$\boldsymbol{A}_i = \begin{bmatrix} 0 & 0 & 1 & 0 \\ 0 & 0 & 0 & 1 \\ -K_{R,p,i} & K_{R,f,i}K_{HR,i} & -K_{R,d,i} & 0 \\ K_{H,f,i}K_{HR,i} & -K_{H,p,i} & 0 & -K_{H,d,i} \end{bmatrix} \tag{19}$$

$$\boldsymbol{E}_i = \begin{bmatrix} 0 & 0 \\ 0 & 0 \\ K_{R,p,i} & 0 \\ 0 & K_{H,p,i} \end{bmatrix}, \boldsymbol{X} = \begin{bmatrix} x_{R,i} \\ x_{H,i} \\ \dot{x}_{R,i} \\ \dot{x}_{H,i} \end{bmatrix}, \boldsymbol{X}_r = \begin{bmatrix} x_{R,r,i} \\ x_{H,r,i} \end{bmatrix}$$

**Table 1**
Control mode during HRC/robot–environment interaction.

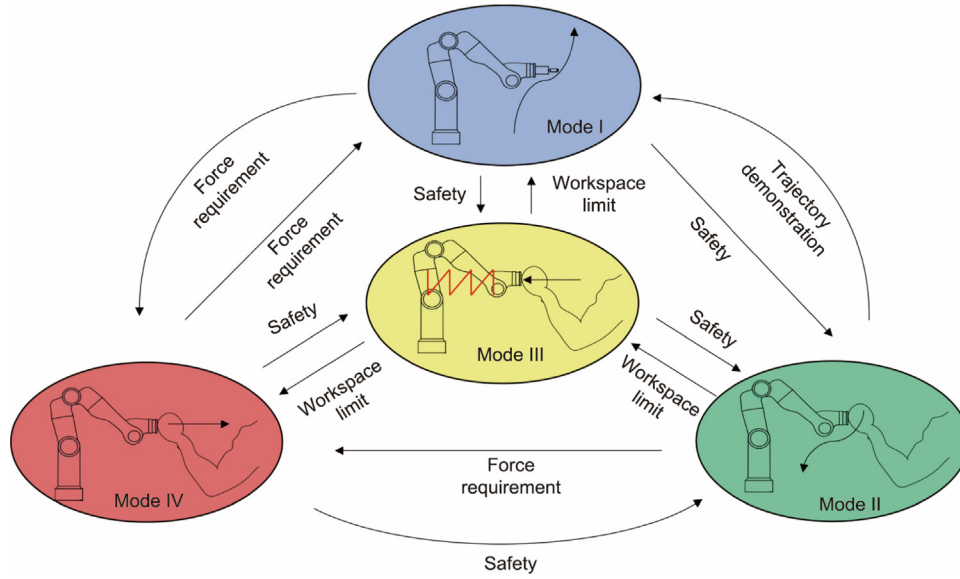| Mode | Control law | Characteristics |
|---|---|---|
| I | $\boldsymbol{K}_{R,p} > 0, \boldsymbol{K}_{R,f} \approx 0$ | $\boldsymbol{x}_{R,eq} \approx \boldsymbol{x}_{R,r}$ or $\boldsymbol{x}_{R,eq} \approx \boldsymbol{x}_{E,r}$ |
| II | $\boldsymbol{K}_{R,p} = 0, \boldsymbol{K}_{R,f} > 0$ | $\boldsymbol{F} = 0$ |
| III | $\boldsymbol{K}_{R,p} > 0, \boldsymbol{K}_{R,f} > 0$ | $\boldsymbol{F} = \boldsymbol{K}_{R,f}^{-1}\boldsymbol{K}_{R,p}\left(\boldsymbol{x}_{R,eq} - \boldsymbol{x}_{R,r}\right)$ |
| IV | $\boldsymbol{K}_{R,p} > 0, \boldsymbol{K}_{R,f} < 0$ | $\boldsymbol{F} = \boldsymbol{K}_{R,f}^{-1}\boldsymbol{K}_{R,p}\boldsymbol{x}_{R,eq}$ |

**Fig. 3.** Switch condition map of different control modes.

where $\dot{X}_i$ is the augment state matrix of human and robot; $A_i$ is the system matrix of human–robot system; $E_i$ is the input matrix; $X_{r,i}$ is the desired trajectory.

To simplify the analysis, only one direction motion ($i$th direction) has been considered.

To further analyze system stability, Lyapunov stability theory is used [47]. A Lyapunov function $V$ is conformed.

$$V = X_i^T P X_i \tag{20}$$

where $P$ is the unit matrix.

The deviation of the Lyapunov function is

$$\dot{V} = \dot{X}_i^T P_i X_i + X_i^T P_i \dot{X}_i = X_i^T (A_i P + P A_i) X_i \tag{21}$$

Eq. (19) is stable when

$$\dot{V} < 0, \quad A_i P + P A_i < 0 \tag{22}$$

Eq. (22) is equivalent to $A_i < 0$, then Eq. (20) is stable when

$$\begin{bmatrix} -K_{R,p,i} + K_{R,f,i}K_{HR,i} & K_{R,f,i}K_{HR,i} \\ K_{H,f,i}K_{HR,i} & -K_{H,p,i} + K_{H,f,i}K_{HR,i} \end{bmatrix} < 0$$
$$\begin{bmatrix} -K_{R,d,i} & 0 \\ 0 & -K_{H,d,i} \end{bmatrix} < 0 \tag{23}$$

Given that $K_{R,d,i}$ and $K_{H,d,i}$ are positive, the stability criterion is

$$\overline{K} = \begin{bmatrix} -K_{R,p,i} + K_{R,f,i}K_{HR,i} & K_{R,f,i}K_{HR,i} \\ K_{H,f,i}K_{HR,i} & -K_{H,p,i} + K_{H,f,i}K_{HR,i} \end{bmatrix} < 0 \tag{24}$$

The eigen value of $\overline{K}$ is

$$\lambda(\overline{K}) = -\frac{1}{2}(-K_{R,p,i} + K_{R,f,i}K_{HR,i} - K_{H,p,i} + K_{H,f,i}K_{HR,i}) \pm$$
$$\frac{1}{2}\sqrt{[-K_{R,p,i} + K_{R,f,i}K_{HR,i} - (-K_{H,p,i} + K_{H,f,i}K_{HR,i})]^2 + 4K_{R,f,i}K_{HR,i}K_{H,f,i}K_{HR,i}} \tag{25}$$

The criterion of the negative definition of $\overline{K}$ is

$$\lambda(\overline{K}) < 0$$
$$-K_{R,p,i}K_{H,p,i} + (K_{R,p,i}K_{H,f,i} + K_{H,p,i}K_{R,f,i})K_{HR,i} < 0 \tag{26}$$

Eq. (26) gives the stability criterion of the HRI. If the switch parameter $\theta_{mod,i} \in [0, \pi]$, then the stability criterion is

$$(K_{H,f,i}\sin\theta_{mod,i} + K_{H,p,i}\cos\theta_{mod,i})K_{HR,i} - K_{H,p,i}\sin\theta_{mod,i} < 0 \tag{27}$$

Eq. (27) shows the stability criterion of the switch system.

**Interaction force of HR system.** When the interaction system is stable, we can calculate the interaction force in the equilibrium position.

In Mode I, the equilibrium force is

$$F = K_{HR}(x_{R,r} + x_{H,eq})$$
$$\text{with } x_{R,eq} = x_{R,r} \tag{28}$$
$$x_{H,eq} = (K_{H,p} - K_{H,f}K_{HR})^{-1}(K_{H,f}K_{HR}x_{R,r} + K_{H,p}x_{H,r})$$

where $x_{H,eq}$ is the equilibrium position of the human in Cartesian space.

In this mode, the robot will reach the desired position. The interaction force is only related to the resistance of the human arm.

In Mode II, the interaction force is $F = 0$. The robot follows the trajectory of the human arm,

$$x_{R,eq} = -x_{H,eq} = -x_{H,r} \tag{29}$$

In Modes III and IV, the interaction force is

$$\begin{bmatrix} x_{R,eq} \\ x_{H,eq} \end{bmatrix} = \begin{bmatrix} K_{R,p} - K_{R,f}K_{HR} & -K_{R,f}K_{HR} \\ -K_{H,f}K_{HR} & K_{H,p} - K_{H,f}K_{HR} \end{bmatrix}^{-1} \begin{bmatrix} K_{R,p}x_{R,r} \\ K_{H,p}x_{H,r} \end{bmatrix}$$
$$F = K_{HR}(x_{R,eq} + x_{H,eq}) \tag{30}$$

In this case, the interaction force depends on $x_{R,r}$ and $x_{H,r}$. The robot has a positive stiffness, and the external force can make the robot deviate from the desired position.

In Mode IV, the robot is with negative stiffness. The robot will move toward the direction of the external force, which results in a larger external force and may tend to unstable. Therefore, mode IV cannot be used alone. It works together with Modes I, II, or III, and to protect the robot from large interaction force.

## 4. Simulation study

In this part, the HRC framework is studied by simulation. To simplify the analysis, we consider the one direction motion of the human arm and the robot. The dynamics of the robot and the human arm are

$$\ddot{x}_R = -K_{R,p}(x_R - x_{R,r}) - K_{R,d}(\dot{x}_R - \dot{x}_{R,r}) + K_{R,f}F$$
$$\ddot{x}_H = -K_{H,p}(x_H - x_{H,r}) - K_{H,d}\dot{x}_H + K_{H,f}F \qquad (31)$$

where $K_{H,p}$, $K_{H,d}$, and $K_{H,f}$ are 10, 50, and 10, respectively; $K_{R,p}$ is changed within 0–10; $K_{R,f}$ is changed within −5 to 10.

The interaction force between the human and robot is

$$F = K_{HR}(x_R + x_H) \qquad (32)$$

where $K_{HR}$ is 30.

The stability map and interaction force map are given in Fig. 4 for HRI. The interaction system is stable in Modes I, II, and III. In Mode IV, the negative stiffness may result in unstable interaction. The interaction force increases when $K_{R,f}$ is decreased. In Mode IV, the interaction force increases rapidly. If the system becomes unstable, then the interaction force approaches infinite. Fig. 5 shows the increase of the interaction force with varied $\theta_{mod}$.

The following simulation shows the dynamic response of the HR coupled system with switched modes. Under the safety principle, the mode switch condition is triggered by the interaction force to protect humans. When the desired position of the robot increases with time, the interaction force continually increased. To eliminate the interaction force, the control mode is varied from IV to III, and finally to II, as shown in Fig. 6.

If the system is initially under the drag and drop mode, then a workspace limitation is necessary to prevent the robot to the dangerous region. Thus, the switch condition is based on the workspace limitation. If the position is out of the limited workspace, then the control mode is switched from Mode II to III and can be further switched to Mode IV against the human motion. Fig. 7 illustrates the interaction force and the position of the robot in this situation. As the desired position of the human arm continuously increased, an oscillation of the HR coupled system occurs because the control mode is continuously switched between Modes IV and III.

The use of the fuzzy switch law in Eq. (17) to reduce the oscillation of the system is possible. When the mode switch condition is triggered, the system is not suddenly changed to the new mode. As the switch time duration is defined as $T$, the switch parameter changes slowly with time, and the sudden force change can be avoided, as shown in Fig. 8. The switch time duration should be set in advance. Short switch time duration may result in sudden force change, whereas long switch time duration delays response speed of the robot. The user should select the suitable switch time duration according to the task requirement.
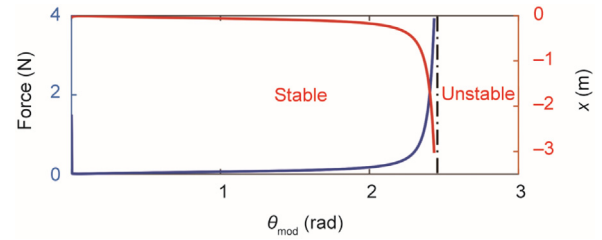


Fig. 5. The interaction force and the equilibrium position of the robot with the increase of $\theta_{mod}$.
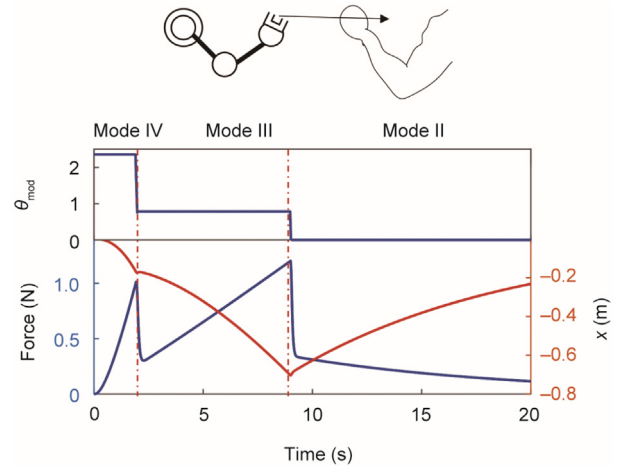


Fig. 6. The interaction force and displacement of the robot when the switch mode is based on the safety principle.
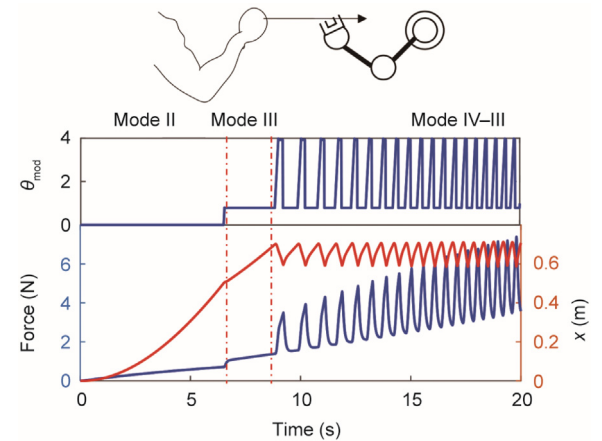


Fig. 7. The interaction force and displacement of the robot when the switch mode is based on the workspace limitation.
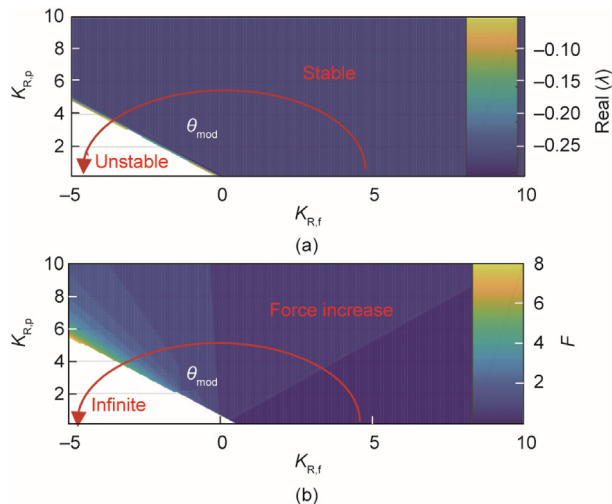
For a specific peg-in-hole assembling task, the interaction occurs within the human, the robot, and the workpiece. At the beginning, the human arm drags the robot to the assembly workstation, where Mode II is selected. When the peg workpiece touches the hole workpiece, the control mode is switched to Mode III. The robot can place the peg workpiece into the hole workpiece through the peg-in-hole constraint, as shown in Fig. 9.

## 5. HRC assembly experiment

In this part, HRC assembling experiments are conducted. An HRC assembly cell is illustrated in Fig. 10. A universal robot 5
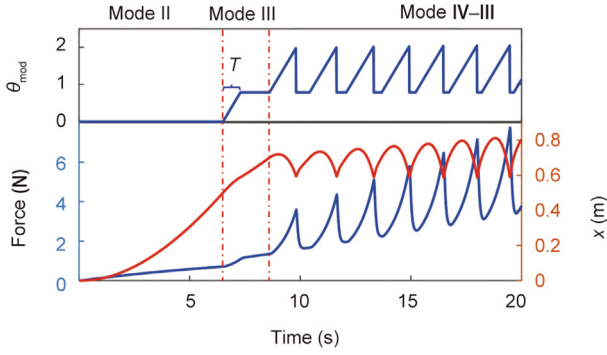


Fig. 4. Characteristic map during HRI with changed $K_{R,p}$ and $K_{R,f}$. (a) Stability map; (b) interaction force.

**Fig. 8.** The interaction force and displacement of the robot when the switch mode is based on the workspace limitation, where the fuzzy switch rule is used.
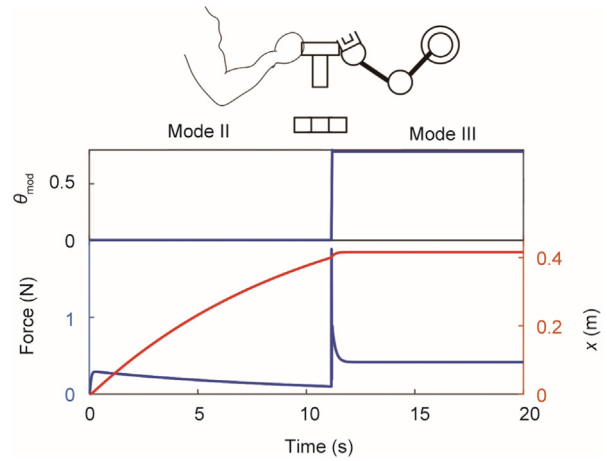


**Fig. 9.** The interaction force and displacement of the robot when the switch mode is based on the task requirement.
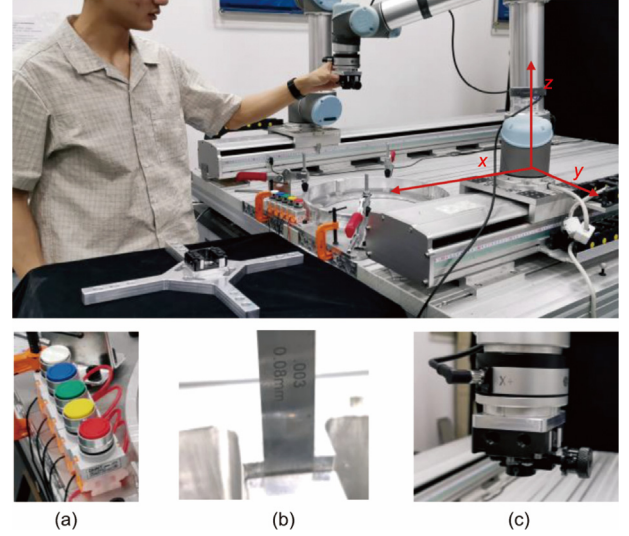


**Fig. 10.** The HRC assembly cell. (a) The switch button to select the interaction mode; (b) the tolerance between the support beam and ring workpieces; (c) the force sensor with a quick-change chuck.

(UR5) is controlled by the robot operation system (ROS). A six-dimension force sensor is added at the end of the robot arm to measure the interaction force. A switch button is connected with the robot control system, and the human can switch the control mode by different switch buttons.

In the first assembly task, a support beam should be inserted into a ring structure, where the support beam is 2 kg, and the assembling tolerance is 0.08 mm because of the manufacturing requirement. Due to the high tolerance, finishing the assembly task manually or by full automation is difficult.

To finish a special assembling work, the HRC assembling strategy is used, where the switch condition is set according to the human command or force criterion. In the HRC assembling, the human is good at adapting the environment. The human can help the robot find the location of the workpiece or lead the robot to the assembling station. The robot is good at carrying a heavy load or performing the high-precision motion.

The control input is the speed in the Cartesian space of the robot.

Translation:

$$u_\xi = k_\xi \sin\theta_{\mathrm{mod}} \ (\xi - \xi_{\mathrm{r}}) + d_\xi \dot{\xi} + k_\xi \cos\theta_{\mathrm{mod}} f_\xi, \xi \in x, y, z \tag{33}$$

Rotation:

$$u_\varsigma = k_\varsigma \sin\theta_{\mathrm{mod}} \ (\varsigma - \varsigma_{\mathrm{r}}) + d_\varsigma \dot{\varsigma} + k_\varsigma \cos\theta_{\mathrm{mod}} \tau_\varsigma, \varsigma \in \alpha, \beta, \gamma$$

where $u_\xi$ is the input speed in $\xi$ direction; $\xi_{\mathrm{r}}$ is the desired position; $d_\xi$ is the damping coefficient; $k_\xi$ is the amplitude of the feedback gain; $f_\xi$ is the external force; $u_\varsigma$ is the input speed in $\varsigma$ direction; $k_\varsigma$ is the amplitude of the feedback gain; $d_\varsigma$ is the damping coeffi-

cient; $\varsigma_{\mathrm{r}}$ is desired angle; $\tau_\varsigma$ is the external torque; $\xi$ is the position in $x, y, z$ and $\dot{\xi}$ is the speed; $\varsigma$ is the angle in $\alpha, \beta, \gamma$ and $\dot{\varsigma}$ is the angular speed.

To compensate for the gravity force of the workpiece, the external force is

$$f_\xi = f_{\xi,\mathrm{m}} - f_{\xi,0}, \tau_\varsigma = \tau_{\varsigma,\mathrm{m}} - \tau_{\varsigma,0} \tag{34}$$

where $f_{\xi,\mathrm{m}}$ and $\tau_{\varsigma,\mathrm{m}}$ are the measured force and torque, respectively; $f_{\xi,0}$ and $\tau_{\varsigma,0}$ are the initial force and torque when the workpiece is carried by the robot, respectively.

The whole workflow is shown in Table 2, and Fig. 11 shows the process and the recording of data during HRC assembling. The whole assembling process was retained for 50 s. In the beginning, Mode II is used. The robot is dragged by the human to find the support beam. In this case, the motion direction and the measured force are in the same direction.

When the robot is near the support beam, Mode IV is used to obtain a large interaction force. In this case, the motion and the force are in opposite directions. A large interaction force is generated when the end-effector touches the workpiece. The interaction force is around 80 N. By doing this, the support beam is docked in the quick-change chuck tightly. Once the crtical force is reached, the control mode is switched to Mode III automatically. Notably, the mode does not directly switched to Mode II. The reason is that the robot may jump out from the assmebly station due to large interaction force.

Additional load is added in the robot when the support beam is connected to the robot end-effector. Thus, the robot is first at Mode

**Table 2**
Workflow of HRC assembly.

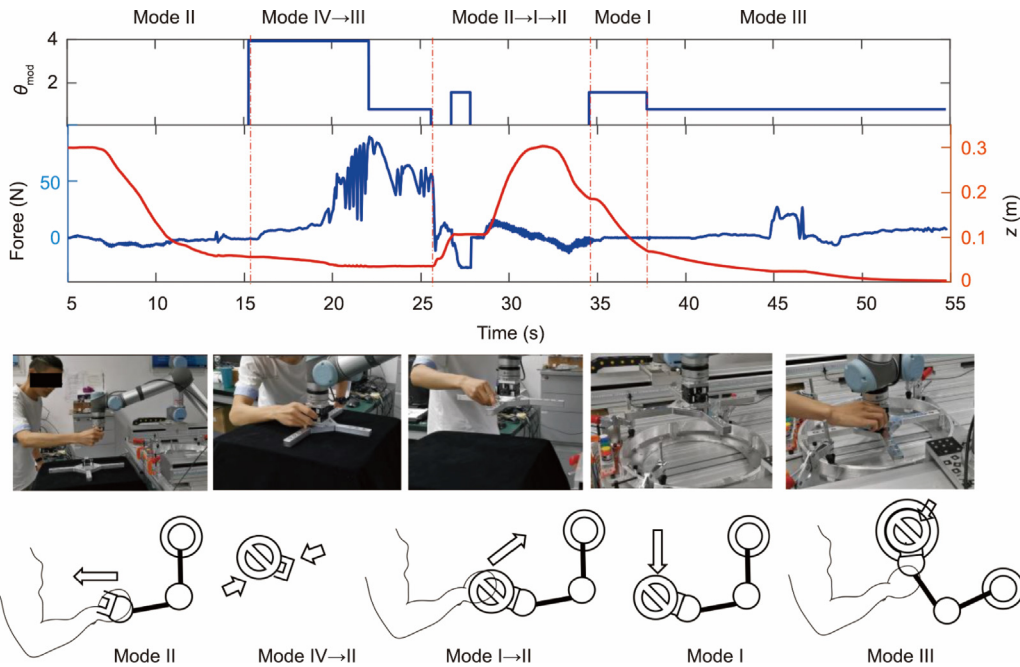| Step | Mode | Target |
|---|---|---|
| 1 | Mode II | Human guides the robot to the position of the support beam |
| 2 | Mode IV→III | Robot is docked with the support beam |
| 3 | Mode II→ I→II | Gravity force compensation, and human guides the robot to the assembly work station |
| 4 | Mode I | Robot transports the support beam near the ring workpiece |
| 5 | Mode III | Robot inserts the support beam to the ring workpiece |

**Fig. 11.** The process and recording data during HRC assembling.

I, and the force sensor measures and compensates the initial force and torque using Eq. (34). Then, the control mode is switched to Mode II. The human can drag the workpiece to the assembly workstation. Later, the control mode is switched to Mode I, and the robot places the support beam down.

Considering that the absolute accuracy of the robot is approximately 0.2 mm, it cannot finish the assembly task with 0.08 mm tolerance only with the position control. Thus, a positive impedance control mode is used in the insertion stage.

In the rotation direction, assembling torque should be avoided.

$$u_\alpha = d_\alpha \dot{\alpha} + k_\alpha \tau_\alpha, u_\beta = d_\beta \dot{\beta} + k_\beta \tau_\beta \quad (35)$$

where $u_\alpha$ and $u_\beta$ are the input speed in $\alpha$ and $\beta$ directions, respectively. $d_\alpha$ and $d_\beta$ are the damping coefficients, $k_\alpha$ and $k_\beta$ are the torque feedbacks, $\tau_\alpha$ and $\tau_\beta$ are the torques. $\dot{\alpha}$ and $\dot{\beta}$ are the speed in $\alpha$ and $\beta$ directions, respectively.

In $z$ direction, the robot moves down only when the vertical force and the torque approach zero.

$$u_z = k_z(z - z_r) + d_z \dot{z} + k_{z,f} f_z + k_{z,\tau} (|\tau_\alpha| + |\tau_\beta|) \quad (36)$$

where $u_z$ is the input speed in $z$ direction; $z$ and $z_r$ are the state and desired value, respectively; $d_z$ is the damping coefficient; $k_z$ is the position feedback; $k_{z,f}$ and $k_{z,\tau}$ are the force and torque feedback gains, respectively; $f_z$ is the interaction force in $z$ direction; the value of $z_r = z_0 - v_0 t$ declines slowly with time.

In $x$ and $y$ directions, the interaction force restrains the motion of the robot.

$$\begin{aligned} u_x &= k_x(x - x_r) + d_x \dot{x} + k_{x,f} f_x + k_\alpha \tau_\alpha \\ u_y &= k_y(y - y_r) + d_y \dot{y} + k_{y,f} f_y + k_\beta \tau_\beta \end{aligned} \quad (37)$$

where $u_x$ and $u_y$ are the input speed in $x$ and $y$ directions, respectively; $x$ and $y$ are the current positions; $x_r$ and $y_r$ are the estimated center of the ring structure; $d_x$ and $d_y$ are the damping coefficients; $k_x$ and $k_y$ are the position feedback; $k_{x,f}$ and $k_{y,f}$ are the force feedback; $k_\alpha$ and $k_\beta$ are the torque feedback.

When the support beam is out of the ring workpiece, the human can push the robot to the insertion position. When the support beam is in the ring workpiece, the interaction force restrains the

robot to find an accurate assembling position. When the torque approaches zero, the robot moves in the $z$ direction and inserts the support beam into the ring workpiece without resistance. The assembling motion trajectory in the insertion stage is given in Fig. 12, where the final assembling accuracy can reach 0.08 mm.

The second experiment indicates the application of the negative impedance control mode. Interference fits are those for which the inside component is larger than the outside component prior to assembly. Large interaction force is required to accomplish an interference assembly. Thus, the negative impedance control mode is used to achieve large interaction force. The workflow of HRC interference assembly is given in Table 3. Fig. 13 shows the experimental environment and motion trajectory of the robot. In the beginning, the robot is in Mode II, and the human can drag the robot to the workstation. Next, the mode is switched to Mode IV, and the robot pushes the pin into the hole. The critical force is set 80 N. When critical force is reached, the robot switches to Mode I automatically, and the interaction force is maintained at 80 N for a moment. Then, the human can switch the control mode to Mode II through the switch button and drags the robot to the next workstation. Fig. 14 shows the force and displacement in the $z$ direction of the robot. The interference assembling can be finished through
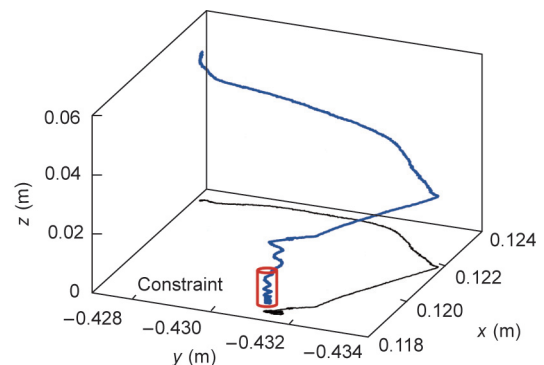


**Fig. 12.** The motion trajectory of the robot in the insertion stage.

**Table 3**
Workflow of HRC interference assembly.

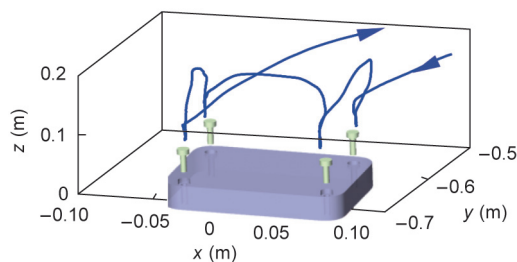| Step | Mode | Target |
| --- | --- | --- |
| 1 | Mode II | Human guides the robot to the workstation |
| 2 | Mode IV→II | Robot pushes the pin into the hole |
| 3 | Mode II | Human guides the robot to the nest workstation |



**Fig. 13.** The experimental environment and motion trajectory of the robot for HRC interference assembly.
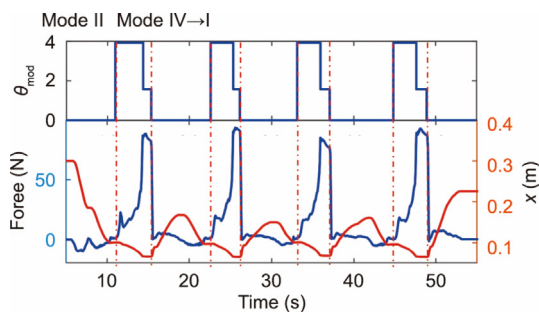


**Fig. 14.** The force and displacement in z direction of the robot for HRC interference assembly.

HRC within 50 s. The experiment shows that the human and robot are companions even when Mode IV is used.

The experiments show that different control modes can be easily switched by the user command or force cretirion, and the HRC assembly has high assembling accuracy and can adapt to complex assembling tasks.

## 6. Conclusions

In this paper, the HRC for robot assembling is studied where four control modes, namely, position control, drag and drop, positive impedance control, and negative impedance control, are proposed. The HRC framework can be established on the basis of the four control modes. The switch condition map is studied to show the transformation relationship among different modes.

The stability of the HR coupled system with different control modes is analyzed. HRC assembling experiments are conducted on a UR5 robot. In the first experiment, the peg-in-hole assembly can be finished within 50 s under the HRC framework where the assembling tolerance is 0.08 mm. The second experiment indicates the application of the negative impedance control mode. The maximum interaction force reaches 80 N for the interference fit. Experiments show that the HRC assembly has the complementary advantages of humans and robots and is efficient in finishing complex assembly tasks. Currently, the switch rule of the HRC framework is mainly based on human commands. In the future, the intelligent switch law based on human intention will be studied.

## Acknowledgments

## Compliance with ethics guidelines

Xingwei Zhao, Yiming Chen, Lu Qian, Bo Tao, and Han Ding declare that they have no conflict of interest or financial conflicts to disclose.

## Appendix A. Supplementary data

Supplementary data to this article can be found online at https://doi.org/10.1016/j.eng.2022.08.022.

## References

[1] De Santis A, Siciliano B, De Luca A, Bicchi A. An atlas of physical human–robot interaction. Mechanism Mach Theory 2008;43(3):253–70.
[2] Li Y, Ge SS. Human–robot collaboration based on motion intention estimation. IEEE/ASME Trans Mechatron 2014;19(3):1007–14.
[3] Day CP. Robotics in industry—their role in intelligent manufacturing. Engineering 2018;4(4):440–5.
[4] Wang B. The future of manufacturing: a new perspective. Engineering 2018;4 (5):722–8.
[5] Krüger J, Lien TK, Verl A. Cooperation of human and machines in assembly lines. CIRP Ann 2009;58(2):628–46.
[6] Ding H, Schipper M, Matthias B. Optimized task distribution for industrial assembly in mixed human–robot environments—case study on IO module assembly. In: Proceedings of 2014 IEEE International Conference on Automation Science and Engineering (CASE); 2014 Aug 18–22; Taipei, China. IEEE; 2014. p. 19–24.
[7] Bley H, Reinhart G, Seliger G, Bernardi M, Korne T. Appropriate human involvement in assembly and disassembly. CIRP Ann 2004;53(2):487–509.
[8] Bonilla BL, Asada HH. A robot on the shoulder: coordinated human–wearable robot control using Coloured Petri Nets and Partial Least Squares predictions. In: Proceedings of 2014 IEEE International Conference on Robotics and Automation (ICRA); 2014 May 31–Jun 7; Hong Kong, China. IEEE; 2014. p. 119–25.
[9] Liu C, Tomizuka M. Modeling and controller design of cooperative robots in workspace sharing human–robot assembly teams. In: Proceedings of 2014 IEEE/RSJ International Conference on Intelligent Robots and Systems; 2014 Sep 14–18; Chicago, IL, USA. IEEE; 2014. p. 1386–91.
[10] Roveda L, Magni M, Cantoni M, Piga D, Bucca G. Human–robot collaboration in sensorless assembly task learning enhanced by uncertainties adaptation via Bayesian optimization. Robot Auton Syst 2021;136:103711.
[11] Jiang J, Huang Z, Bi Z, Ma X, Yu G. State-of-the-art control strategies for robotic PiH assembly. Robot Comput Integr Manuf 2020;65:101894.
[12] Realyvásquez-Vargas A, Arredondo-Soto KC, García-Alcaraz JL, Márquez-Lobato BY, Cruz-García J. Introduction and configuration of a collaborative robot in an assembly task as a means to decrease occupational risks and increase efficiency in a manufacturing company. Robot Comput Integr Manuf 2019;57:315–28.
[13] Ramirez-Amaro K, Beetz M, Cheng G. Transferring skills to humanoid robots by extracting semantic representations from observations of human activities. Artif Intell 2017;247:95–118.
[14] Huang B, Li M, De Souza RL, Bryson JJ, Billard A. A modular approach to learning manipulation strategies from human demonstration. Auton Robots 2016;40(5):903–27.

[15] Yang C, Zeng C, Liang P, Li Z, Li R, Su CY. Interface design of a physical human–robot interaction system for human impedance adaptive skill transfer. IEEE Trans Autom Sci Eng 2018;15(1):329–40.

[16] Yang C, Zeng C, Fang C, He W, Li Z. A DMPs-based framework for robot learning and generalization of humanlike variable impedance skills. IEEE/ASME Trans Mechatron 2018;23(3):1193–203.

[17] Mörtl A, Lawitzky M, Kucukyilmaz A, Sezgin M, Basdogan C, Hirche S. The role of roles: physical cooperation between humans and robots. Int J Robot Res 2012;31(13):1656–74.

[18] Gillespie RB, Colgate JE, Peshkin MA. A general framework for robot control. IEEE Trans Robot Autom 2001;17(4):391–401.

[19] Erden MS, Billard A. Robotic assistance by impedance compensation for hand movements while manual welding. IEEE Trans Cybern 2016;46(11):2459–72.

[20] Jarrassé N, Sanguineti V, Burdet E. Slaves no longer: review on role assignment for human–robot joint motor action. Adapt Behav 2014;22(1):70–82.

[21] Musić S, Hirche S. Control sharing in human–robot team interaction. Annu Rev Contr 2017;44:342–54.

[22] Khoramshahi M, Billard A. A dynamical system approach to task-adaptation in physical human–robot interaction. Auton Robots 2019;43(4):927–46.

[23] Zhang R, Lv Q, Li J, Bao J, Liu T, Liu S. A reinforcement learning method for human–robot collaboration in assembly tasks. Robot Comput Integr Manuf 2022;73:102227.

[24] Hogan N. Impedance control: an approach to manipulation: part II—implementation. J Dyn Sys Meas Control 1985;107(1):8–16.

[25] Zhao X, Tao B, Qian L, Yang Y, Ding H. Asymmetrical nonlinear impedance control for dual robotic machining of thin-walled workpieces. Robot Comput Integr Manuf 2020;63:101889.

[26] Cremer S, Das SK, Wijayasinghe IB, Popa DO, Lewis FL. Model-free online neuroadaptive controller with intent estimation for physical human–robot interaction. IEEE Trans Robot 2020;36(1):240–53.

[27] Burdet E, Osu R, Franklin DW, Milner TE, Kawato M. The central nervous system stabilizes unstable dynamics by learning optimal impedance. Nature 2001;414(6862):446–9.

[28] Li Y, Ganesh G, Jarrassé N, Haddadin S, Albu-Schaeffer A, Burdet E. Force, impedance, and trajectory learning for contact tooling and haptic identification. IEEE Trans Robot 2018;34(5):1170–82.

[29] Chen X, Wang N, Cheng H, Yang C. Neural learning enhanced variable admittance control for human–robot collaboration. IEEE Access 2020;8:25727–37.

[30] Roveda L, Maskani J, Franceschi P, Abdi A, Braghin F, Molinari Tosatti L, et al. Model-based reinforcement learning variable impedance control for human–robot collaboration. J Intell Robot Syst 2020;100(2):417–33.

[31] Zhao X, Han S, Tao B, Yin Z, Ding H. Model-based actor–critic learning of robotic impedance control in complex interactive environment. IEEE Trans Ind Electron 2022;69(12):13225–35.

[32] Jarrassé N, Charalambous T, Burdet E. A framework to describe, analyze and generate interactive motor behaviors. PLoS One 2012;7(11):e49945.

[33] Li Y, Carboni G, Gonzalez F, Campolo D, Burdet E. Differential game theory for versatile physical human–robot interaction. Nat Mach Intell 2019;1(1):36–43.

[34] Gervasi R, Mastrogiacomo L, Franceschini F. A conceptual framework to evaluate human–robot collaboration. Int J Adv Manuf Technol 2020;108(3):841–65.

[35] Mukherjee D, Gupta K, Chang LH, Najjaran H. A survey of robot learning strategies for human–robot collaboration in industrial settings. Robot Comput Integr Manuf 2022;73:102231.

[36] Xing H, Torabi A, Ding L, Gao H, Li W, Mushahwar VK, et al. Human–robot collaboration for heavy object manipulation: Kinesthetic teaching of the role of wheeled mobile manipulator. In: Proceedings of 2021 IEEE/RSJ International Conference on Intelligent Robots and Systems (IROS); 2021 Sep 27–Oct 1; Prague, Czech Republic. IEEE; 2021. p. 2962–9.

[37] Kim W, Peternel L, Lorenzini M, Babič J, Ajoudani A. A human–robot collaboration framework for improving ergonomics during dexterous operation of power tools. Robot Comput Integr Manuf 2021;68:102084.

[38] Peternel L, Tsagarakis N, Caldwell D, Ajoudani A. Robot adaptation to human physical fatigue in human–robot co-manipulation. Auton Robots 2018;42(5):1011–21.

[39] Gopinath V, Johansen K, Derelöv M, Gustafsson Å, Axelsson S. Safe collaborative assembly on a continuously moving line with large industrial robots. Robot Comput Integr Manuf 2021;67:102048.

[40] Villani V, Pini F, Leali F, Secchi C. Survey on human–robot collaboration in industrial settings: safety, intuitive interfaces and applications. Mechatronics 2018;55:248–66.

[41] Ajoudani A, Zanchettin AM, Ivaldi S, Albu-Schäffer A, Kosuge K, Khatib O. Progress and prospects of the human–robot collaboration. Auton Robots 2018;42(5):957–75.

[42] Matheson E, Minto R, Zampieri EGG, Faccio M, Rosati G. Human–robot collaboration in manufacturing applications: a review. Robotics 2019;8(4):100.

[43] Liu H, Wang L. Gesture recognition for human–robot collaboration: a review. Int J Ind Ergon 2018;68:355–67.

[44] Liu H, Wang L. Remote human–robot collaboration: a cyber–physical system application for hazard manufacturing environment. J Manuf Syst 2020;54:24–34.

[45] Khatib O. A unified approach for motion and force control of robot manipulators: the operational space formulation. IEEE J Robot Autom 1987;3(1):43–53.

[46] Buerger SP, Hogan N. Complementary stability and loop shaping for improved human–robot interaction. IEEE Trans Robot 2007;23(2):232–44.

[47] Branicky MS. Stability of hybrid systems: State of the art. In: Proceedings of the 36th IEEE Conference on Decision and Control. San Diego, CA, USA: IEEE; 1997 Dec 12. p. 120–5.